ELSEVIER

Coordination Chemistry Reviews
208 (2000) 309–320

COORDINATION CHEMISTRY REVIEWS

www.elsevier.com/locate/ccr

Changes in excited-state character of $[M(L_1)(L_2)(CO)_2(\alpha\text{-diimine})]$ (M = Ru, Os) induced by variation of L_1 and L_2

J. van Slageren [a], F. Hartl [a], D.J. Stufkens [a,*], D.M. Martino [b], H. van Willigen [b]

[a] *Institute of Molecular Chemistry, Universiteit van Amsterdam, Nieuwe Achtergracht 166, NL-1018 WV Amsterdam, The Netherlands*

[b] *Department of Chemistry, University of Massachusetts at Boston, Boston, MA 02125, USA*

Received 21 September 1999; accepted 24 February 2000

Contents

Abstract 309
1. Introduction 310
2. Results and discussion 311
   2.1 Electronic absorption and resonance Raman spectra 311
   2.2 Excited state properties 315
   2.3 Time-resolved FT-EPR spectra of photo-generated methyl radicals 317
Acknowledgements 319
References 319

Abstract

The character of the lowest excited state of the d^6-complexes $[M(L_1)(L_2)(CO)_2(\alpha\text{-diimine}]$ (M = Ru, Os) varies with L_1 and L_2. In the case of $[Ru(Cl)(Me)(CO)_2(\alpha\text{-diimine})]$ it has predominant metal-to-ligand charge transfer (MLCT) character. For $[M(SnPh_3)_2CO)_2(\alpha\text{-diimine})]$ (M = Ru, Os), having two axial $SnPh_3$ ligands, it has $\sigma(Sn–M–Sn)\pi^*(\alpha\text{-diimine})$ (Sigma-Bond-to-Ligand Charge Transfer, SBLCT) character. In a glass at 90 K the emission lifetimes of the $[Ru(SnPh_3)_2(CO)_2(\alpha\text{-diimine})]$ complexes are nearly a thousand times longer than those of the corresponding $[Ru(Cl)(Me)(CO)_2(\alpha\text{-diimine})]$ compounds, although their

* Corresponding author. Tel.: +31-20-5256451; fax: +31-20-5256456.
E-mail address: stufkens@anorg.chem.uva.nl (D.J. Stufkens).

PII: S0010-8545(00)00333-7

emission energies are very similar. In fact, these lifetimes are extremely long (e.g. $\tau = 1070$ μs for $[Ru(SnPh_3)_2(CO)_2(4,4'\text{-dimethyl-}2,2'\text{-bipyridine})]$) for a CT state. Although replacement of Ru by Os decreases both the emission energy and lifetime of complexes such as $[M(bpy)_3]^{2+}$ (M = Ru, Os), only the emission lifetime decreases in the case of the $[M(SnPh_3)_2CO)_2(\alpha\text{-diimine})]$ compounds. The latter effect is due to the increase of spin-orbit coupling (SOC), the influence of which could thus be studied without taking into account any energy-gap-law effect. Preliminary photophysical data are presented for $[Pt(SnPh_3)_2(Me)_2(i\text{-Pr-DAB})]$, which has very similar excited state properties as the corresponding Ru- and Os-complexes. Replacement of a $SnPh_3$ ligand by a methyl group to give $[Ru(Me)(SnPh_3)(CO)_2(i\text{-Pr-DAB})]$ increases the photoreactivity of the complex. The weaker Ru–Me bond is broken homolytically and the formation of methyl radicals was studied in detail with FT-EPR spectroscopy.

Keywords: Ru; Os; α-Diimine complexes; Emission; Resonance Raman; MLCT states; SBLCT states; FT-EPR; Methyl radicals

1. Introduction

In recent years our group has studied in detail the influence of co-ligands (L, L_1 and L_2) on the excited state properties of the d^6 complexes $[M'(L)(CO)_3(\alpha\text{-diimine})]$ (M′ = Mn, Re) [1–11] and $[M(L_1)(L_2)(CO)_2(\alpha\text{-diimine})]$ (M = Ru, Os) [9,12–21], in which the co-ligands are halides (X) [1–4,12–14], alkyl or benzyl groups [5–9,15,16], or metal fragments [10,11,13,17–21]. Variation of L, L_1 or L_2 often causes a dramatic change of the lowest excited state character with a concomitant strong effect on the photophysical and photochemical properties.[22] For instance, replacement of L = Cl in $[Re(L)(CO)_3(\alpha\text{-diimine})]$ by L = I, causes the lowest excited state character to change from mainly metal-to-ligand charge transfer (MLCT) to halide-to-ligand charge transfer (XLCT) [4]. For $L = SnPh_3$, Et or Bz this state has instead sigma-bond-to-ligand charge transfer (SBLCT or σπ*) character [7,10,11]. In that case electron density has been transferred from the σ(Re–L) orbital to π*(α-diimine) with a concomitant weakening of the Re–L bond. For $L = SnPh_3$ this bond is still fairly strong in the excited state [11], whereas it is broken efficiently if L = Et or Bz [7].

A similar behavior has been observed for the complexes $[Ru(L_1)(L_2)(CO)_2(\alpha\text{-diimine})]$. For L_1 = Cl, L_2 = Me (Fig. 1(a)) the lowest excited state has predominant MLCT character [12–14], for L_1 = I, L_2 = Me it is XLCT [12–14] and for L_1 = X, $L_2 = i$-Pr or Bz it is SBLCT or σπ* [15,16]. If both L_1 and L_2 are bound to Ru by a high-lying σ orbital (Fig. 1(b) and (c)) it is again a SBLCT or σπ* state [17,18,20,21]. However, in that case the σ orbital is delocalized with contributions from 5p(Ru), the antisymmetric combination of the σ orbitals of L_1 and L_2, and π*(α-diimine) [18,20]. On irradiation, the weaker σ bond (Ru–L_1 or Ru–L_2) is broken. For instance, excitation of $[Ru\{Mn(CO)_5\}(Me)(CO)_2(\alpha\text{-diimine})]$ gives rise to homolysis of the Ru–Mn bond and formation of $Mn(CO)_5$ radicals [17], whereas methyl radicals are formed upon excitation of $[Ru(Me)(SnPh_3)(CO)_2(\alpha\text{-diimine})]$

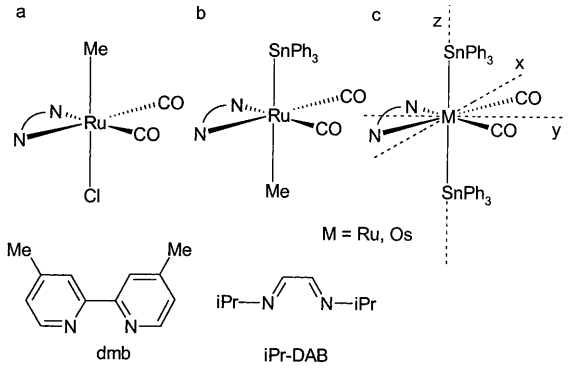

Fig. 1. Schematic structures of the complexes and the α-diimine ligands used as well as the chosen orientation of axes.

(Fig. 1(b)) [19]. This particular behavior of the SBLCT complexes and their synthetic accessibility makes it possible to photogenerate different types of radicals, which can, e.g. be used as initiators of addition polymerization reactions. Even the complexes $[Ru(SnPh_3)_2(CO)_2(\alpha\text{-diimine})]$ (Fig. 1(c)) are photoreactive at room temperature, in spite of the relatively strong Ru–Sn bond [19].

Here we present the absorption and emission properties of the complexes $[Ru(Cl)(Me)(CO)_2(\alpha\text{-diimine})]$ and $[Ru(SnPh_3)_2(CO)_2(\alpha\text{-diimine})]$ in a glass at 90 K. In addition, we discuss the influence of the central metal atom M (Ru, Os) and the α-diimine on the emission properties of the complexes $[M(SnPh_3)_2(CO)_2(\alpha\text{-diimine})]$ and present the time-resolved FT-EPR spectra of the methyl radicals produced by photoexcitation of $[Ru(Me)(SnPh_3)(CO)_2(i\text{-Pr-DAB})]$.

2. Results and discussion

2.1. Electronic absorption and resonance Raman spectra

The complexes $[Ru(Cl)(Me)(CO)_2(i\text{-Pr-DAB})]$ (**1**) and $[Ru(SnPh_3)_2(CO)_2(i\text{-Pr-DAB})]$ (**2**) (for numbering see Table 2) are good representatives of the two series of complexes having a lowest MLCT and SBLCT state, respectively. Their absorption spectra in benzene are shown in Fig. 2.

The spectrum of **1** shows a band at 450 nm ($\varepsilon = 1710\ M^{-1}\ cm^{-1}$), which has been assigned to a transition with predominant MLCT character [12]. This assignment was based on its solvatochromism, and on the resonance Raman spectra obtained by excitation into this transition. In addition, the time-resolved IR and Raman spectra confirmed the MLCT character of the lowest excited state [14]. On the other hand, DFT calculations on the model complexes $[Ru(Cl)(Me)(CO)_2(H\text{–DAB})]$ [23] and $[Ru(Cl)(SnH_3)(CO)_2(H\text{–DAB})]$ [20] show that the transition originates from an orbital having mixed $d_\pi(Ru)$–$p_\pi(Cl)$ character. The spectrum of **2** shows bands at 525 nm ($\varepsilon = 6050\ M^{-1}\ cm^{-1}$) and 400 nm ($\varepsilon = 450$

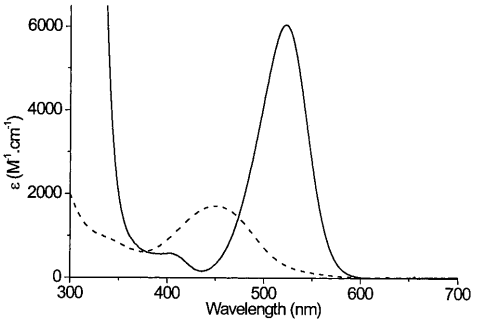

Fig. 2. Electronic absorption spectra of **1** (dashed) and **2** (solid) in benzene.

M^{-1} cm^{-1}), respectively. In order to understand the electronic structure of **2** and to assign these absorption bands, DFT MO calculations were performed on the model complex $[Ru(SnH_3)_2(CO)_2(H–DAB)]$ [18]. A qualitative MO scheme is shown in Fig. 3 (the chosen orientation of axes is depicted in figure 1), while the characters and energies of the relevant MOs are presented in Table 1.

Thus, the HOMO is only weakly bonding between Ru and the axial SnH_3 ligands and there is a strong $\sigma–\pi^*$ interaction, i.e. delocalization of the electron density from the SnH_3 ligands to H–DAB in both the HOMO and LUMO. This delocalization is evident from the strong scalar coupling of the $^{117/119}Sn$ nuclei to the imine protons in the ^1H-NMR spectra of **2** [24] and from the large hyperfine splitting constants a_{Sn} in the EPR spectrum of the radical anion of **2** [18]. The absorption band of **2** at 525 nm is assigned to the HOMO → LUMO (SBLCT) transition. Due

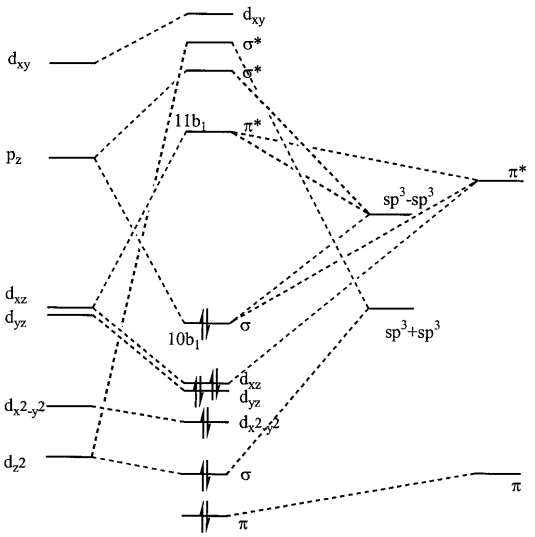

Fig. 3. Qualitative MO scheme of $[Ru(SnH_3)_2(CO)_2(H–DAB)]$.

Table 1
Characters (%) and energies of the relevant MOs of $[Ru(SnH_3)_2(CO)_2(H–DAB)]$ [18]

Orbital	Description	E (eV)	Ru	SnH_3	H–DAB	CO
$11b_1$ (LUMO)	π*	−3.984	11% d_{yz}	27% $3a_1$	61% $2b_1$	
$10b_1$ (HOMO)	σ(Sn–Ru–Sn)	−5.924	15% p_z	42% $3a_1$	27% $2b_1$	9% 2π
$9b_1$	d(Ru)	−7.009	53% d_{yz}	27% 3e	6% $2b_1$	7% 2π
$16a_1$	σ(Sn–Ru–Sn)	−7.820	11% 5s, 53% d_{z2}	7% $2a_1$, 34% $3a_1$		

to the strong σ–π* interaction this transition is rather intense (Fig. 2). However, although this transition formally has SBLCT character, the shift of electron density from the axial SnH_3 ligands to H–DAB, as derived from the changes in Mulliken populations, is rather small [20]. As a result of the strong σ–π* interaction, the ruthenium d-orbitals can only mix very weakly with π*(H–DAB) in $[Ru(SnH_3)_2(CO)_2(H–DAB)]$ (Table 1). The $4d_{yz}(Ru) \rightarrow \pi^*$(*i*-Pr–DAB) (MLCT) transition of **2** is therefore weak, which explains the very low intensity of the 400 nm MLCT band of this complex (Fig. 2).

Substitution of the non-aromatic *i*-Pr-DAB ligand in **2** by dmb (yielding complex **3**) hardly affects the energy of the SBLCT transition (λ_{max} merely shifts from 515 to 521 nm in THF), although the π* orbital of dmb is appreciably higher in energy. This effect is most likely due to a more extensive σ–π* delocalization in the case of the *i*-Pr–DAB complex, giving rise to more overlap stabilization and an increase of the HOMO–LUMO energy gap. As mentioned above, the SBLCT transition of **2** only causes a small shift of electron density due to the strong σ–π* interaction. Therefore, the energy of this transition hardly depends on the solvent polarity. Accordingly, the solvatochromic shift of this transition [$\nu(CH_3CN)$–ν(toluene)] is only 565 cm^{-1} for **2**. The solvatochromic shift of complex **3** is larger (1430 cm^{-1}) in agreement with a less extensive σ–π* delocalization for the dmb complex [25].

In order to further establish the differences in character of the lowest-energy transitions of **1** and **2**, their resonance Raman (rR) spectra were recorded. Such spectra exhibit resonance enhancement of Raman intensity for those vibrations which are most strongly coupled to the allowed electronic transition in which excitation takes place. The rR spectra of **1** and **2**, dispersed in KNO_3, are shown in Fig. 4. The spectrum of **1** is rather simple, it shows only rR effects for ν_s(CN) of the *i*-Pr–DAB ligand at 1573 cm^{-1}, for ν_s(Ru–CO) at 492 cm^{-1}, and for ν_s(CO) at 2017 cm^{-1}. This spectrum demonstrates that the electronic transition affects the CN-bonds of the *i*-Pr-DAB ligand in addition to the CO and Ru–CO bonds, in agreement with its charge transfer character. The rR intensity of ν_s(CO) is rather low, which implies that the Ru–CO π backbonding is hardly affected by this transition. This agrees with the mixed MLCT/XLCT character of this transition derived from DFT MO calculations [23]. It is noteworthy that the spectrum does not show a rR effect for ν(CC) of the central C–C bond of the *i*-Pr-DAB ligand, although occupation of its lowest π* orbital is expected not only to weaken the C–N bonds, but at the same time to strengthen the C–C bond. The origin of this effect is currently under investigation.

The rR spectrum of **2** obtained by excitation into its 525 nm SBLCT band differs appreciably from that of **1**. First of all, the spectrum shows weaker rR effects than that of **1** which means that the normal coordinates of **2** are less affected by the SBLCT transition than those of **1** by the MLCT transition. More and different Raman bands of **2** are resonantly enhanced implying that more bonds and angles are affected than for **1**. Thus, both ν_s(Ru–CO) and ν_s(CO) are absent, showing that the electron density at Ru is hardly affected by this transition, in agreement with the results of the DFT calculations (Table 1). The frequency of ν_s(CN) is nearly 100 cm^{-1} lower than in the case of **1**, indicating that the $\sigma-\pi^*$ interaction of **2** is much stronger than the ($d_\pi-\pi^*$) π-backbonding of **1**. The differences in electronic transitions of **1** and **2** are also manifested by the observation of rR effects for ν(CC) of *i*-Pr-DAB at 1282 cm^{-1} and for deformation modes of this ligand at 953 and 838 cm^{-1} in the case of **2**.

Fig. 4 also presents the rR spectra of [$Os(SnPh_3)_2(CO)_2$(*i*-Pr–DAB)] (**6**) and [$Pt(SnPh_3)_2(Me)_2$(*i*-Pr–DAB)] (**10**). According to theoretical and spectroscopic studies of [$Pt(Me)_4$(*i*-Pr–DAB)] [26], the lowest energy transition of this complex has SBLCT character, and this is also true for [$Pt(SnPh_3)_2(Me)_2$(*i*-Pr–DAB)] [27]. According to their rR spectra (Fig. 4) there is indeed a close analogy between the electronic structures of complexes **2**, **6** and **10**, although the extent of $\sigma-\pi^*$ interaction varies from one compound to another. For instance, the rR spectra of complex **2** and its Os-derivative (**6**) are very much alike, showing only small differences in relative intensities, not in frequencies [25]. The rR spectrum of [$Pt(SnPh_3)_2(Me)_2$(*i*-Pr-DAB)] (**10**) shows again the rR effects for ν_s(CN) and ν(CC) which are typical for an SBLCT transition [27]. However, in this case the distortion of the *i*-Pr-DAB ligand, reflected in rR effects for its deformation modes at ca. 950 and 840 cm^{-1}, is very weak. This variation of the rR intensity of the deformation modes has been observed before and appears to be connected with the variation in charge transfer character of the electronic transition [28].

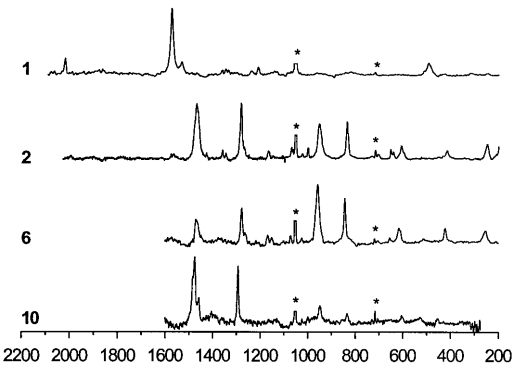

Fig. 4. Resonance Raman spectra of (from top to bottom) [Ru(Cl)(Me)(CO)2(*i*-Pr–DAB)] (**1**), [$Ru(SnPh_3)_2(CO)_2$(*i*-Pr–DAB)] (**2**), [$Os(SnPh_3)_2(CO)_2$(*i*-Pr–DAB)] (**6**) and [$Pt(SnPh_3)(Me)_2$(*i*-Pr–DAB)] (**10**). Spectra were obtained at r.t. by excitation of the complexes as KNO_3 pellets into their lowest-energy electronic transition. Asterisks denote nitrate bands.

2.2. Excited state properties

Most complexes with a lowest SBLCT state undergo homolysis of a metal–axial ligand bond. Which reaction takes place and how efficient it is mainly depends on the strengths of these bonds. For instance, whereas complex **2** photodecomposes at room temperature with a quantum yield of 0.23 (in DCM) [19], the corresponding Os-complex [$Os(SnPh_3)_2(CO)_2$(*i*-Pr-DAB)] (**6**) is virtually photostable, due to the stronger Os–Sn bond [25]. Such an increase of bond strength is expected since transition metal–Sn bonds become stronger for heavier metals. For instance, the energy of the M–Sn bond in [$Cp(CO)_3M$–$SnMe_3$] (M = Cr, Mo, W) increases from 223 (M = Cr) to 297 (M = Mo) and 316 kJ mol^{-1} (M = W) [29]. This increase in photostability is reflected in a longer excited state lifetime at room temperature (r.t.) (1 μs for **2**, 1.5 μs for **6**) although a shorter lifetime is expected (and in fact observed at low temperature, vide infra) due to a stronger spin-orbit coupling for the Os-complex.

The emission spectra of several of the complexes in a 2-MeTHF glass at 90 K, under which conditions they are photostable, are presented hereafter. The time-resolved FT-EPR spectra of the methyl radicals, obtained by irradiation of [$Ru(Me)(SnPh_3)(CO)_2$(*i*-Pr-DAB)], are reported in the next section.

The emission data are collected in Table 2, while the absorption, emission and excitation spectra of the representative complex [$Ru(SnPh_3)_2(CO)_2$(dmb)] (**3**) are presented in Fig. 5. Although complex **1** absorbs at much shorter wavelength than **2**, it emits at nearly the same energy. In fact, the difference in energy between the maxima of absorption and emission (from the corresponding triplet state) (ΔE_{abs-em}) of **2** is about half the value found for **1**. This means that **2** is much less distorted in its lowest excited state than **1**, which agrees with the above mentioned rR data. This difference in distortion has a large effect on the rate of nonradiative decay (k_{nr}), which determines emission lifetimes of these complexes. In fact, k_{nr} decreases by almost three orders of magnitude, with a corresponding increase in the emission lifetime ($\tau = 0.3$ μs for **1** and 264 μs for **2**). The distortion of the complex in its excited state decreases even more when the *i*-Pr-DAB ligand in **2** is replaced

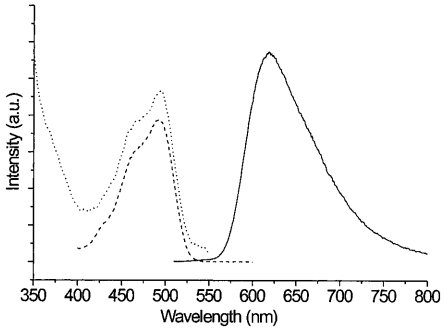

Fig. 5. Emission (solid line), absorption (dotted) and excitation (dashed) spectra of [$Ru(SnPh_3)_2(CO)_2$(dmb)] (**3**) in a 2-MeTHF glass at 90 K.

Table 2
Emission data of the complexes in a 2-MeTHF glass at 90 K

	Excited state	Complex	λ_{abs} (nm)	λ_{em} (nm)	ΔE_{abs-em} (cm^{-1})	τ (μs)	Φ (%)	k_r (10^2 s^{-1})	k_{nr} (10^2 s^{-1})
1	MLCT	$Ru(Cl)(Me)(CO)_2$(*i*-Pr–DAB)	387	650	10455	0.3	0.034	11.4	38440
2	SBLCT	$Ru(SnPh_3)_2(CO)_2$(*i*-Pr–DAB)	495	670	5277	264	1.5	0.55	37
3	SBLCT	$Ru(SnPh_3)_2(CO)_2$(dmb)	495	604	3646	1070	5.7	0.62	10
4	SBLCT	$Ru(SnPh_3)_2(CO)_2$(*p*An-BIAN)	595	821	4626	68			
5	SBLCT	$Ru[RuCp(CO)_2]_2(CO)_2$ (*i*-Pr–DAB)	593	855	5168	9			
6	SBLCT	$Os(SnPh_3)_2(CO)_2$(*i*-Pr–DAB)	478	655	5653	32	0.58	1.83	313
7	SBLCT	$Os(SnPh_3)_2(CO)_2$(dmb)	485	589	3641	221	3.4	1.51	42
8	MLCT	$Ru(bpy)_3^{2+}$	455	582	4800	5.1	32.8	643	1318
9	MLCT	$Os(bpy)_3^{2+}$	476	775	8000	0.77	7.6	987	12000
10	SBLCT	$Pt(SnPh_3)_2(Me)_2$(*i*-Pr–DAB)	615	809	3899	1.2			

by the much more rigid dmb (**3**). This is reflected in a further decrease of ΔE_{abs-em} and k_{nr}, and a concomitant increase of τ. In fact, $\tau = 1070$ μs, which is extremely high for a CT state [25].

The absorption and emission energies of the complexes having a lowest SBLCT state can be tuned rather easily by varying the α-diimine or the axial ligands. For instance, replacement of the *i*-Pr–DAB ligand in **2** by *p*An-BIAN [bis(*p*-anisylimino)acenaphthene] to give $[Ru(SnPh_3)_2(CO)_2(pAn\text{-}BIAN)]$ (**4**), which has a much lower-lying π* level, shifts the emission maximum from 670 to 821 nm (Table 2) [25]. Similarly, replacement of the $SnPh_3$ ligands in **2** by the more strongly σ-donating $RuCp(CO)_2$ groups to give $[Ru\{RuCp(CO)_2\}_2(CO)_2(i\text{-}Pr\text{-}DAB)]$ (**5**), causes a shift of the emission from 670 to 855 nm [30]. Despite their low emission energies, the SBLCT states of **4** and **5** still have rather long lifetimes. This makes these SBLCT complexes promising candidates for NIR emitters, provided they can be made completely photostable at r.t.

Replacement of Ru by Os hardly influences the absorption and emission energies (see Table 2), indicating again that the central metal atom is hardly involved in the frontier orbitals [25]. This contrasts with the behavior of, e.g. the complexes $[M(bpy)_3]^{2+}$ (M = Ru, Os; complex **8** and **9**, respectively) where the replacement of Ru by Os shifts both the absorption and emission to lower energies due to the higher energy of the metal-d_π orbital involved in the main MLCT transition (see Table 2). However, although the emission energies and excited state distortions of complexes **2** and **6**, as well as of **3** and **7**, are very much alike, their emission lifetimes are very different. This can only be caused by an increase of spin-orbit coupling (SOC) going from Ru to Os, which reduces the emission lifetime. It is exceptional that the influence of SOC alone is observed in this case without interference from other influences such as energy-gap-law effects [25].

The recently prepared complex $[Pt(SnPh_3)_2(Me)_2(i\text{-}Pr\text{-}DAB)]$ (**10**) emits at low temperatures with a lifetime of 1.2 μs (see Table 2) [27]. This lifetime is not very long, but comparable to that of the corresponding Os complex **6**, taking into account the much lower emission energy of **10**.

2.3. Time-resolved FT-EPR spectra of photo-generated methyl radicals

FT-EPR spectroscopy can be used to detect and identify transient radicals without using a spin trap [31]. After a $\pi/2$ pulse (in the microwave region of the electromagnetic spectrum), the free induction decay is recorded, which represents the time domain spectrum of the radical present at the time of the microwave pulse. By Fourier transformation the frequency domain spectrum is obtained. One limitation of this technique is the deadtime of the instrument caused by cavity ring down. Due to this deadtime, which amounts to 100 ns for the equipment used in this work, the FT-EPR technique cannot be used for radicals having fast decaying FIDs (free induction decays), i.e. for those having broad linewidths in the frequency domain. In practice this generally precludes the detection of metal containing radicals.

The FT-EPR spectra of the methyl radicals obtained by excitation of [Ru(Me)($SnPh_3$)($CO)_2$(*i*-Pr-DAB)] at various excitation wavelengths, are presented in Fig. 6. These spectra show signals in absorption and emission and differ in their intensity patterns. In order to explain these patterns we must realize that, due to the short time delay between radical generation and measurements (typically between 10 ns and 1 μs), the electron spin is not at thermal equilibrium. Processes which create non-Boltzmann electron spin distributions are collectively known as CIDEP (chemically induced dynamic electron polarization) effects [31].

It has been shown that the polarization patterns observed in the spectra of Fig. 6 are due to a combination of the ST_0 and ST_{-1} radical pair mechanisms [32]. The ST_0 RPM is caused by the difference in precession frequency of the two unpaired electrons of the radical pair and usually involves a three-step process [33,34]. After generation of a contact radical pair, the radicals diffuse apart, by which the mixing between the singlet (S) and triplet T_0 states of the radical pair becomes effective. Finally, the radicals may re-encounter in the solvent cage. The ST_0 RPM depends on the nuclear spin state so that relative intensities of hyperfine components in the spectrum will differ from those found at thermal equilibrium. Spin polarization generated by the ST_0 RPM shows up in the spectrum as emission peaks at low field and as enhanced absorption peaks at high field, provided the radicals are produced from a triplet excited state precursor. In the ST_{-1} RPM, spin polarization is generated by mixing of the singlet and T_{-1} component of the triplet radical pair state and leads to a hyperfine dependent emissive spectrum [33,35].

It is noteworthy that the polarization pattern depends on the wavelength of excitation [36]. Such an effect has not been observed for any of the radicals produced by excitation of the related complexes [Ru(I)(R)($CO)_2$(α-diimine)] (R = *i*-Pr, Bz) and [Re(R)$CO)_3$(α-diimine)] (R = Et, *i*-Pr) [9]. Upon low-energy irradiation (λ_{irr} = 440, 532 nm) the EPR spectra show a clear emission/absorption polarization pattern with net overall emission (E*/A). On higher-energy irradiation (λ_{irr} = 308,

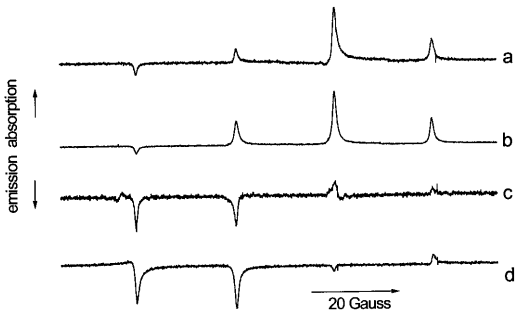

Fig. 6. FT-EPR spectra of methyl radicals obtained by irradiation of [Ru(Me)($SnPh_3$)($CO)_2$(*i*-Pr–DAB)] in toluene with (a) 308 nm; (b) 355 nm; (c) 440 nm and (d) 532 nm laser light. The signals are the averages produced by 400 laser shots, except spectrum (c) (4000 laser shots). Absorption signals point up.

355 nm), an emission/absorption polarization pattern with net overall absorption (E/A*) is observed. This difference is explained as follows: At higher energy, excitation does not take place anymore into the first SBLCT band but into the second SBLCT band, which belongs to a transition from a σ(Sn–Ru–Me) orbital (composed of a $4d_{z^2}$(Ru) orbital and the symmetric combination of the σ orbitals of the axial Me and $SnPh_3$ ligands) to π*(*i*-Pr–DAB) [20]. The difference in polarization pattern suggests that the radical formation is a very fast, activationless process from different non-equilibrated excited states. The complexes [Ru(I)(R)$(CO)_2$(α-diimine)] (R = *i*-Pr, Bz) and [Re(R)$CO)_3$(α-diimine)] (R = Et, *i*-Pr) do not have such a second SBLCT state. The fact that the FT-EPR spectra of the radicals formed from these complexes do not show a wavelength-dependent polarization pattern, supports our interpretation.

Acknowledgements

Many thanks are owed to Dr C.J. Kleverlaan (University of Amsterdam) for preliminary FT-EPR measurements on [Ru(Me)$(SnPh_3)(CO)_2$(iPr-DAB)] and to Dr A. Klein (University of Stuttgart) for his collaboration on the Pt-compounds. Financial support for this work was provided by the Council for Chemical Sciences of the Netherlands Organization for Scientific Research (CW-NWO) and the Division of Chemical Sciences, Office of Basic Energy Sciences of the US Department of Energy (DE-FG02-84ER-13242).

References

[1] G.J. Stor, S.L. Morrison, D.J. Stufkens, A. Oskam, Organometallics 13 (1994) 2641.
[2] C.J. Kleverlaan, F. Hartl, D.J.J. Stufkens, Photochem. Photobiol. A: Chem. 103 (1997) 231.
[3] B.D. Rossenaar, D.J. Stufkens, A. Vlček Jr., Inorg. Chim. Acta 247 (1996) 247.
[4] B.D. Rossenaar, D.J. Stufkens, A. Vlček Jr., Inorg. Chem. 35 (1996) 2902.
[5] B.D. Rossenaar, D.J. Stufkens, A. Oskam, J. Fraanje, K. Goubitz, Inorg. Chim. Acta 247 (1996) 215.
[6] B.D. Rossenaar, M.W. George, F.P.A. Johnson, D.J. Stufkens, J.J. Turner, A. Vlček Jr., J. Am. Chem. Soc. 117 (1995) 11582.
[7] B.D. Rossenaar, C.J. Kleverlaan, M.C.E. van de Ven, D.J. Stufkens, A. Vlček Jr., Chem. Eur. J. 2 (1996) 228.
[8] C.J. Kleverlaan, D.J. Stufkens, I.P. Clark, M.W. George, J.J. Turner, D.M. Martino, H. van Willigen, A. Vlček Jr., J. Am. Chem. Soc. 120 (1998) 10871.
[9] C.J. Kleverlaan, D.M. Martino, H. van Willigen, D.J. Stufkens, A. Oskam, J. Phys. Chem. 100 (1996) 18607.
[10] R.R. Andréa, W.G.J. de Lange, D.J. Stufkens, A. Oskam, Inorg. Chem. 28 (1989) 318.
[11] B.D. Rossenaar, E. Lindsay, D.J. Stufkens, A. Vlček Jr., Inorg. Chim. Acta 250 (1996) 5.
[12] H.A. Nieuwenhuis, D.J. Stufkens, A. Oskam, Inorg. Chem. 33 (1994) 3212.
[13] H.A. Nieuwenhuis, D.J. Stufkens, A. Vlček Jr., Inorg. Chem. 34 (1995) 3879.
[14] H.A. Nieuwenhuis, D.J. Stufkens, R.A. McNicholl, A.H.R. Al-Obaidi, C.G. Coates, S.E.J. Bell, J.J. McGarvey, J. Westwell, M.W. George, J.J. Turner, J. Am. Chem. Soc. 117 (1995) 5579.

[15] H.A. Nieuwenhuis, M.C.E. van de Ven, D.J. Stufkens, A. Oskam, K. Goubitz, Organometallics 14 (1995) 780.
[16] C.J. Kleverlaan, D.J. Stufkens, J. Photochem. Photobiol. A: Chem. 116 (1998) 109.
[17] H.A. Nieuwenhuis, A. van Loon, M.A. Moraal, D.J. Stufkens, A. Oskam, K. Goubitz, J. Organomet. Chem. 492 (1995) 165.
[18] M.P. Aarnts, M.P. Wilms, K. Peelen, J. Fraanje, K. Goubitz, F. Hartl, D.J. Stufkens, E.J. Baerends, A. Vlček Jr., Inorg. Chem. 35 (1996) 5468.
[19] M.P. Aarnts, D.J. Stufkens, A. Vlček Jr., Inorg. Chim. Acta 266 (1997) 37.
[20] M.P. Aarnts, D.J. Stufkens, M.P. Wilms, E.J. Baerends, A. Vlček Jr., I.P. Clark, M.W. George, J.J. Turner, Chem. Eur. J. 2 (1996) 1556.
[21] M.P. Aarnts, M.P. Wilms, D.J. Stufkens, E.J. Baerends, A. Vlček Jr., Organometallics 16 (1997) 2055.
[22] D.J. Stufkens, A. Vlček Jr., Coord. Chem. Rev. 177 (1998) 127.
[23] S. Záliš et al., to be published.
[24] M.P. Aarnts, D.J. Stufkens, A. Oskam, J. Fraanje, K. Goubitz, Inorg. Chim. Acta 256 (1997) 93.
[25] J. van Slageren, D.J. Stufkens, submitted for publication.
[26] W. Kaim, A. Klein, S. Hasenzahl, H. Stoll, S. Záliš, J. Fiedler, Organometallics 17 (1998) 237.
[27] J. van Slageren, S. Záliš, A. Klein, to be published.
[28] R.W. Balk, D.J. Stufkens, A. Oskam, J. Chem. Soc. Dalton Trans. (1982) 275.
[29] D.J. Cardin, S.A. Keppie, M.F. Lappert, M.R. Litzow, T.R. Spalding, J. Chem. Soc. (A) (1971) 2262.
[30] J. van Slageren, F. Hartl, D.J. Stufkens, Eur. J. Inorg. Chem., in press.
[31] H. van Willigen, P.R. Levstein, M.H. Ebersole, Chem. Rev. 93 (1993) 173.
[32] J. van Slageren, D.M. Martino, C.J. Kleverlaan, A.P. Bussandri, H. van Willigen, D.J. Stufkens, submitted for publication.
[33] K.A. McLauchlan, Continuous-Wave Transient Electron Spin Resonance CIDEP, L. Kevan, M.K. Bowman (Eds.), Wiley, New York, 1990, pp. 285–363.
[34] L. Monchik, F.J. Adrian, J. Chem. Phys. 68 (1978) 4376.
[35] C.D. Buckley, K.A. McLauchlan, Chem. Phys. Lett. 137 (1987) 86.
[36] C.J. Kleverlaan, D.M. Martino, J. van Slageren, H. van Willigen, D.J. Stufkens, A. Oskam, Appl. Magn. Res. 15 (1998) 203.